International Journal of Engineering Trends and Technology
ISSN: 2231 – 5381 /doi:10.14445/22315381/IJETT-V70I2P224
Volume 70 Issue 2, 201-213, February, 2022

Original Article

A Ceramic Setting And Firing With Loading And Unloading Via Robots

Benchalak Muangmeesri[1], Dechrit Maneetham[2]

[1]*Technology Management, Valaya Alongkorn Rajabhat University, Pathumthani, Thailand*
[2]*Mechatronics Engineering, Rajamangala University of Technology Thanyaburi, Thailand*

benchalak@vru.ac.th, dechrit_m@rmutt.ac.th

Abstract - *Ceramic surfaces behave the effect of various ceramic fillers to heat treatment of polyethylene-based composites. The temperature of the ceramic during firing is inserted into the hot chamber with high temperatures that have a significant influence on the process. The robot with a four Degree of Freedom (4-DOF) has been designed to set between loading and unloading a ceramic to the chamber. The robot can control the position, speed, and time of the ceramic with loading and unloading of the chamber, as well as able to prevent hazards for workers while picking and catching workpieces from the hot chamber. To load and unload the kiln, the manipulator arm of the robot can insert a ceramic into the hot chamber via a charging hole on the kiln. The robot can also be operated manually and automatically with a ceramic position. Automatic control operation accuracy was estimated position to be within* ± 3 *mm. and able to increase work efficiency in industrial applications.*

Keywords - *Ceramic, Material, Oven, Industrial Robotics.*

I. INTRODUCTION

In general, ceramics change chemically over time, including pre-burn and post-burn materials. Ceramic bodies are very widely in composition, depending on the finished properties required. A common brick might be made from many materials and still have sufficient strength, but the matter of cost requires that it be made of easily accessible clays that will fire at low temperatures. On the other hand, even though the cost is high, fine porcelain must be made of materials that are free from colouring impurities and from which will develop a body of high translucency. It is impossible to make it complete, but nevertheless, it serves its purpose. This method is convenient for compounding, but it does not permit easy comparison of one body with another.

As a means of comparing bodies, it has been customary in Europe to express the body composition on equivalent minerals as first suggested. The materials of minerals analysis. While this method is not used to a great extent in this country, due largely to doubts about the validity of the calculation of the clay substance, it is of considerable value in obtaining a broad view of body compositions. The firing process of ceramic is very complex, and there is always an anti-chemical reaction. All of these variables have a direct and indirect effect. Thus, there must be good control of the burning temperature, which is always important. The aims of firing are then at a higher temperature [3]. In order, glaze ware uses an average firing temperature at about 700-800^0 C (1292-1472^0 F) before a glaze ware is adapted. The average extraction temperature would be estimated at 600-900^0 C (1112-1652^0 F), usually 750-850^0 C (1382-1562^0 F) [4], enamel kiln, which is a muffle kiln or an electric kiln. The temperature will cause a change in a texture that may necessitate a number of such firings as well as the thermal efficiency of periodic kilns depending on many factors such as maximum temperature, temperature uniformity, type of setting, insulation, and heat capacity of the kiln itself. As mentioned above, the ceramic in the kiln has a very high temperature. Therefore, domestic applications must be complete with time, and industrial robotics has been developed to assist in loading and unloading from a stove with a high temperature [5],[7]. At the same time, if the ceramic is heated and waited for a long period to cool in the oven, the waiting time is lost, but if workers pick up the workpiece from a high-temperature oven, it cannot be done either. The kiln operation and industrial robots are interrelated and controlled via automatic temperature control. When the temperature inside the furnace is about 100 degrees, the robot will automatically take out or unload the ceramic workpiece from the furnace. This Research will describe the ceramic with loading and unloading of the chamber, temperature, and kinematics of manipulators. Ceramic setting and tempering are explained in section II. Section III presents the kinematics of robotics for the proposed position control. Section IV experimental results compare the position control with loading and unloading, and conclusions are given in section V.

II. PROPERTIES OF CERAMIC

The clays vary in character over a wide range; some are particularly valuable to the ceramic industry. A cray that is found in the same position as the parent rock from which it was derived is called residual. It is now generally believed that most residual clays are formed by a series of reactions caused by the percolation of groundwater through the mass, aided by many other weathering factors such as freezing. This water is dissolved CO_2 from the air and organic acids from vegetation. In the following equations, the steps in the process are delineated. However, there is no evidence that, in nature, such a step by step process occurs.

hydrolysis $HAISi_3O_8 + KOH = \frac{KAISi_3O_8 + H_2O}{feldspar}$ (1)

desilication $HAISi_3O_8 = \rho \frac{(OH)AISi_2O_5}{pyrophyllite} + SiO_2$ (2)

desilication $HAISi_3O_8 = HAISiO_4 + 2SiO_2$ (3)

hydration $2HAISiO_4 + H_2O = \frac{(OH)_4 AI_2Si_2O_5}{kaolinite}$ (4)

desilication $HAISiO_4 = \frac{HAIO_4}{diaspore} + SiO_2$ (5)

hydration $HAIO_2 + H_2O = \frac{AI(OH)_3}{gibbsite}$ (6)

In Table 1, the parameters of the clay minerals are listed. The particle size of clay is a very important characteristic since it influences many other properties such as plasticity, dry strength, and base exchange capacity.

Table 1. The Parameters of Clays.

Parameters	Symbol	soft clay	stiff clay
Mass density (kg/m^3)	ρ	1,575	1,595
Bulk modulus (kPa)	k	5.7*10^4	9.73*10^4
Shear modulus (kPa)	G	8.4*10^3	15.9*10^3
Poisson's ratio (kPa)	v	0.43	0.42
Electric modulus (kPa)	E	2.4*10^4	4.5*10^4
Cohesion intercept (kPa)	c	45	90
Cohesion (kPa)	c_{sb}	30	45
Normal stiffness (kPa/m)	k_{rp}	4.5*10^4	7.6*10^4
Shear stiffness (kPa/m)	k_s	5*10^2	8*10^2

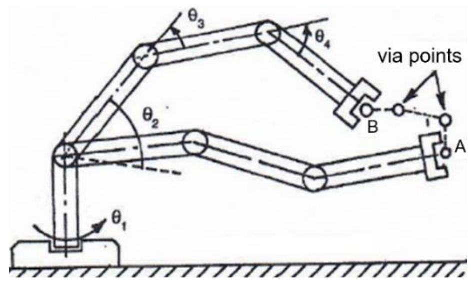

Fig. 1 Shear Stress of Solid and Soft Clay

III. TRAJECTOR GENERATION

A robot can be considered to effector may be provided with a gripper and electromagnet or a spot welding rod. The position and workspace of the frame assigned to the tool concerning the base frame are of primary interest in kinematic [10]

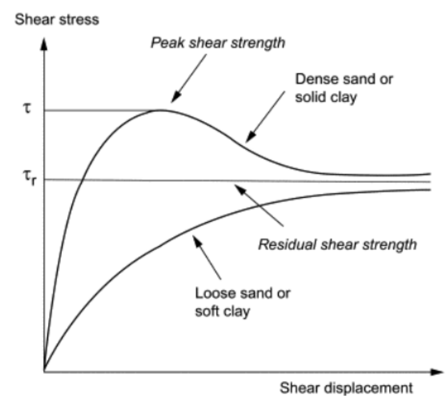

Fig. 2 Industrial robotics and position control

kinematics [10]. The robot needs to move from a point A to some point B and shown in Fig.2, through some exacted moderate points. The workspace of variable $\theta(t)$ time is known as the movement of the robots. A linear motion between the points A B depends on the control and degrees of motion as well as velocities and accelerations [15].

A. FORWARD KINEMATICS

In this Research, the robot has a kind of motion with four degrees of freedom, If the joint angles $\theta_1, \theta_2, \theta_3, \theta_4$ are specified and can control the position and workspace of the gripper [11]. The question of the forward kinematics can be separated as follows:

$$r(t) = f(\theta(t)) \quad (7)$$

with $\theta(t) =$ joint variables

$r(t) =$ cartesian variables

$f(.) =$ non linear function

These conventions have been chosen the Denavit Hartenberg notation [15], the a_i units are oriented from axis $\hat{z}_i$ to axis $\hat{z}_{i+1}$, as measured along the $\hat{x}_i$, the α_i units is the angle from axis $\hat{z}_i$ to axis $\hat{z}_{i+1}$, as measured along the $\hat{x}_i$, the d_i units is oriented from axis $\hat{x}_{i-1}$ to axis $\hat{x}_i$, as measured along the $\hat{z}_i$, the θ_i units is oriented from axis $\hat{x}_{i-1}$ to axis $\hat{x}_i$, as measured along the $\hat{z}_i$. Figure 3. Shown a four-link articulated robotic arm. A rotation $\theta_1,\theta_2,\theta_3,\theta_4$, and frame $\{i\}$ to link frame $\{j\}$ by a translation $\{d_i\}$ can be derived rotation matrix R_{i-1}^{i} through the Eq. (8).

$$R_{i-1}^{i}=\begin{bmatrix}\cos\theta_i & -\sin\theta_i & 0 & b_i\\ \cos\alpha_i\sin\theta_i & \cos\alpha_i\cos\theta_i & -\sin\alpha_i & -d_i\sin\alpha_i\\ \sin\alpha_i\sin\theta_i & \sin\alpha_i\cos\theta_i & \cos\theta_i & d_i\cos\alpha_i\\ 0 & 0 & 0 & 1\end{bmatrix} \tag{8}$$

The schematic geometrical diagram of link frame assignments for the articulated robotics arm is shown in the Figure below.

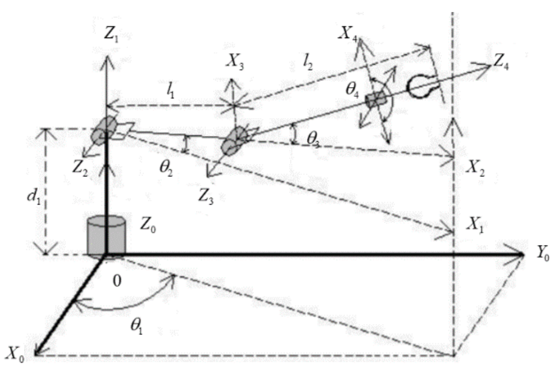

a) Robot arm links and joints

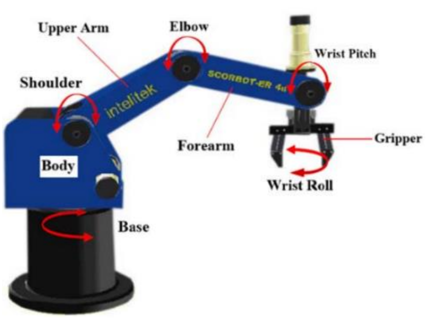

b) Frame assignment

Fig. 3 A four-link the articulated robotic arm

Assign link frames to the mechanism and give the Denavit – Hartenberg parameters are given in Table 2.

Table 2. DH Parameters of 4 DOF Articulated Robotic Arm

Link	α_i	a_i	θ_i	d_i
1	0	0	θ_1	d_1
2	90	0	θ_2	0
3	0	l_1	θ_3	0
4	90	l_2	θ_4	0

The R_{i-1}^{i} is rotation matrix of the transformation matrix as in the following the articulated robotic arm equation.

$$^{0}R_1=\begin{bmatrix}\cos\theta_1 & -\sin\theta_1 & 0 & 0\\ \sin\theta_1 & \cos\theta_1 & 0 & 0\\ 0 & 0 & 1 & d_1\\ 0 & 0 & 0 & 1\end{bmatrix}$$

$$^{1}R_2=\begin{bmatrix}\cos\theta_2 & -\sin\theta_2 & 0 & 0\\ 0 & 0 & -1 & 0\\ \sin\theta_2 & \cos\theta_2 & 0 & 0\\ 0 & 0 & 0 & 1\end{bmatrix}$$

$$^{2}R_3=\begin{bmatrix}\cos\theta_3 & -\sin\theta_3 & 0 & l_1\\ \sin\theta_3 & \cos\theta_3 & 0 & 0\\ 0 & 0 & 1 & 0\\ 0 & 0 & 0 & 1\end{bmatrix}$$

$$^{3}R_4=\begin{bmatrix}\cos\theta_4 & -\sin\theta_4 & 0 & l_2\\ 0 & 0 & -1 & 0\\ \sin\theta_4 & \cos\theta_4 & 0 & 0\\ 0 & 0 & 0 & 1\end{bmatrix}$$

Which makes the articulated robotic arm and calculated the kinematic of robotics. To apply to the industrial robot, the articulated robotic arm is perhaps the simplest to analyze. The link R_{i-1}^{i} for the joint of each link and the adept one robot are as follows:

$$^{0}R_4={}^{0}R_1\,{}^{1}R_2\,{}^{2}R_3\,{}^{3}R_4 \tag{9}$$

$$^{0}R_4=\begin{bmatrix}c_1c_4c_{23}+s_1s_4 & -c_1s_4c_{23}+s_1c_4 & c_1s_{23} & l_2c_1c_{23}+l_1c_1c_2\\ s_1c_4c_{23}-c_1s_4 & -s_1s_4c_{23}-c_1c_4 & s_1s_{23} & l_2s_1c_{23}+l_1s_1c_2\\ c_4s_{23} & -s_4s_{23} & -c_{23} & l_2s_{23}+l_1s_2+d_1\\ 0 & 0 & 0 & 1\end{bmatrix}$$

The case where C_i denotes $\cos(\theta_i)$ and S_i denotes $sin(\theta_i)$. The end-effector position and orientation are achieved.

$$\begin{bmatrix} D_x \\ D_y \\ D_z \end{bmatrix} = \begin{bmatrix} l_2 \cos\theta_1 \cos\theta_2 + l_1 \cos\theta_1 \cos\theta_2 \\ l_1 \sin\theta_1 \cos\theta_{23} + l_1 \sin\theta_1 \cos\theta_2 \\ l_2 \sin\theta_{23} + l_1 \sin\theta_2 + d_1 \end{bmatrix} \quad (10)$$

B. INVERSE KINEMATICS

The inverse kinematics calculations are calculated from the endpoint starting from the gripper, moving the axis downward until the starting point of the robot axis. When robots are in motion, links and manipulators have more complex and more difficult calculations than forwarding kinematics [14]. The inverse kinematics equation is given below.

$$\theta(t) = l_2^{-1}(r(t)) \quad (11)$$

The inverse kinematics problem is the structure and weight of the robot influence the control, and every joint of the robot must be able to handle axial and angular loads. One of the gripper angles θ_4 will make an angle in the pitch angle θ_4 as well as axial control calculation at all the pitch angles θ_{234}. The computing of the gripper angle can define with the following variable.

$$(D_{x0}^4 D_{y0}^4 D_{z0}^4) = (P_x, P_y, P_z) \quad (12)$$

There are the articulated robotic arm equations for all kinematic analysis of this manipulator, is given by

$$l_2 \cos\theta_1 \cos\theta_{23} + l_1 \cos\theta_1 \cos\theta_2 = P_x \quad (13)$$

$$l_2 \sin\theta_1 \cos\theta_{23} + l_1 \cos\theta_1 \cos\theta_2 = P_y \quad (14)$$

$$l_2 \sin\theta_{23} + l_1 \sin\theta_2 + d_1 = P_z \quad (15)$$

$$l_1 \cos\theta_2 + l_2 \cos_{23} = \cos\theta_1 P_x + \sin\theta_1 P_y \quad (16)$$

$$\cos\theta_1 P_y - \sin\theta_1 P_x = 0 \quad (17)$$

$$l_1 + l_2 \cos\theta_3 = \cos\theta_2(\cos\theta_1 P_x) + (P_z - d_1)\sin\theta_2 \quad (18)$$

$$l_2 \sin\theta_3 = -\sin\theta_2(\cos\theta_1 P_x + \sin\theta_1 P_y) + (P_z - d_1)\cos\theta_2 \quad (19)$$

This constraint can be summarized the value of angle θ_1, θ_2 and θ_3 as for the terms of the angle of the articulated robotic arm as follows:

$$\theta_1 = A\tan 2\left(\frac{P_y}{P_x}\right) \quad (20)$$

$$\theta_2 = A\tan 2\left(\frac{(P_z - d_1)(l_1 + l_2\cos\theta_3) - l_2 \sin\theta_3 \sqrt{P_x^2 + P_y^2}}{(P_z - d_1) l_2 \sin\theta_3 + (l_1 + l_2 \cos\theta_3)\sqrt{P_x^2 + P_y^2}}\right) \quad (21)$$

$$\theta_3 = A\tan 2\left(\frac{\pm\sqrt{4 l_1^2 l_2^2 - [(P_z - h)^2 + P_x^2 + P_y^2 - l_1^2 - l_2^2]^2}}{(P_z - d_1)^2 + P_x^2 + P_y^2 - l_1^2 - l_2^2}\right) \quad (22)$$

IV. RESULT AND DISCUSSION

In the experiment, the articulated robotic arm is tested to a ceramic setting with loading and unloading via kiln. A personal computer (PC) and EtherCAT-based control method and the software supported by IEC61131-3 programming standard. The control system consists of a central processing unit (CPU) with card BK1120, the input system section with card KL1408, the output system section with card KL2552 as well as including the optical encoders for control closed-loop system all axis. The control system of the articulated robotic arm is shown in Fig 4.

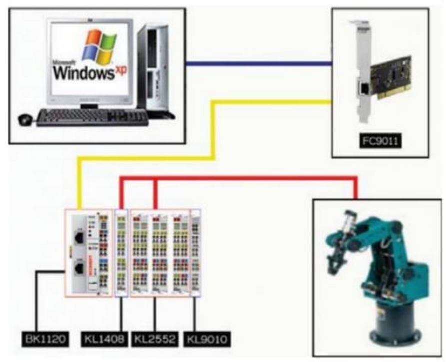

Fig. 4 Control System Configuration

A. CLAY AND GLAZES

As for the term of ceramic firing with clay and glazes. It is very important to control the temperature so as not to make it polished and the workpiece is scratched or broken. Typically the firing temperature is up to 1500^0 C . Clay ingredients include the stoneware clay 52%, ball clay 20%, silica 10%, and feldspar 18%. After the greenware process, the glaze ware process has to be carried out after the initial firing process. There will be many advantages such as preventing absorption, resistance to acid and alkali corrosion, preventing fungal infection, and making beautiful products. The process can be represented as follows:

a) greenware

b) biscuit ware at 1200^{0}C

c) glazes ware at 1200^{0}C

Fig. 5 Clay and Glazes for the potter

B. LOADING AND UNLOADING

Material handling for the kiln is very significant because taking the products with loading and unloading of the kiln at high temperatures is quite dangerous. Especially working with workers will require relatively high working time, and worker fatigue will occur while working. Therefore, it is imperative to have a robotic system to assist in this kind of work in order to achieve quality work and reduce working time.

Fig. 6 Articulated Robot Arm Moving of Loading and Unloading a Ceramic

C. IMULATION OF THE ARTICULATED ROBOT ARM

The forward and inverse kinematics model of the articulated robot arm has been Simulink via toolbox in MATLAB. This refers to the entire revolute space for which the forward and inverse kinematics problem has a solution to determine the position and workspace of the gripper. Suppose the joint angle configuration $\theta_1, \theta_2, \theta_3, \theta_4$ is specified as [0 45^0 0 45^0]. The Simulation of the position and workspace with the gripper is given as follows.

$$\begin{bmatrix} P_x \\ P_y \\ P_z \end{bmatrix} = \begin{bmatrix} 45.2 \\ 0 \\ 20 \end{bmatrix}$$

After that, simulate the robot working program according to the specified angle value. The direction of the movement of the robot in the new position is as follows.

$$\begin{bmatrix} P_x \\ P_y \\ P_z \end{bmatrix} = \begin{bmatrix} 47.3127 \\ 0 \\ 66.1127 \end{bmatrix}$$

```
>> Rob.fkine([0 0 0 0 0])

ans =

    1.0000         0         0   45.2000
         0   -1.0000   -0.0000   -0.0000
         0    0.0000   -1.0000   20.0000
         0         0         0    1.0000

>> Rob.fkine([0 pi/4 0 pi/4 0])

ans =

    0.0000   -0.0000    1.0000   47.3127
    0.0000   -1.0000   -0.0000    0.0000
    1.0000    0.0000   -0.0000   66.1127
         0         0         0    1.0000
```

Fig. 7 Simulink with 'Rob.fkine' in MATLAB Software

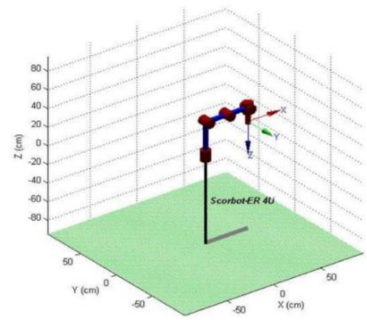

a) Joint Angle at [0 0 0 0]

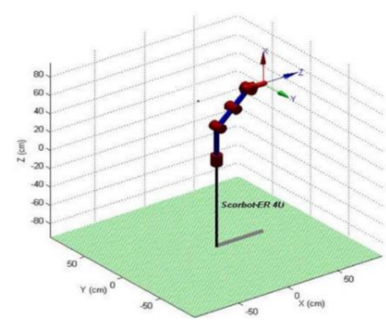

b) joint angle at [0 45 0 45]

Fig. 8 Simulink of Joint Angle Configuration

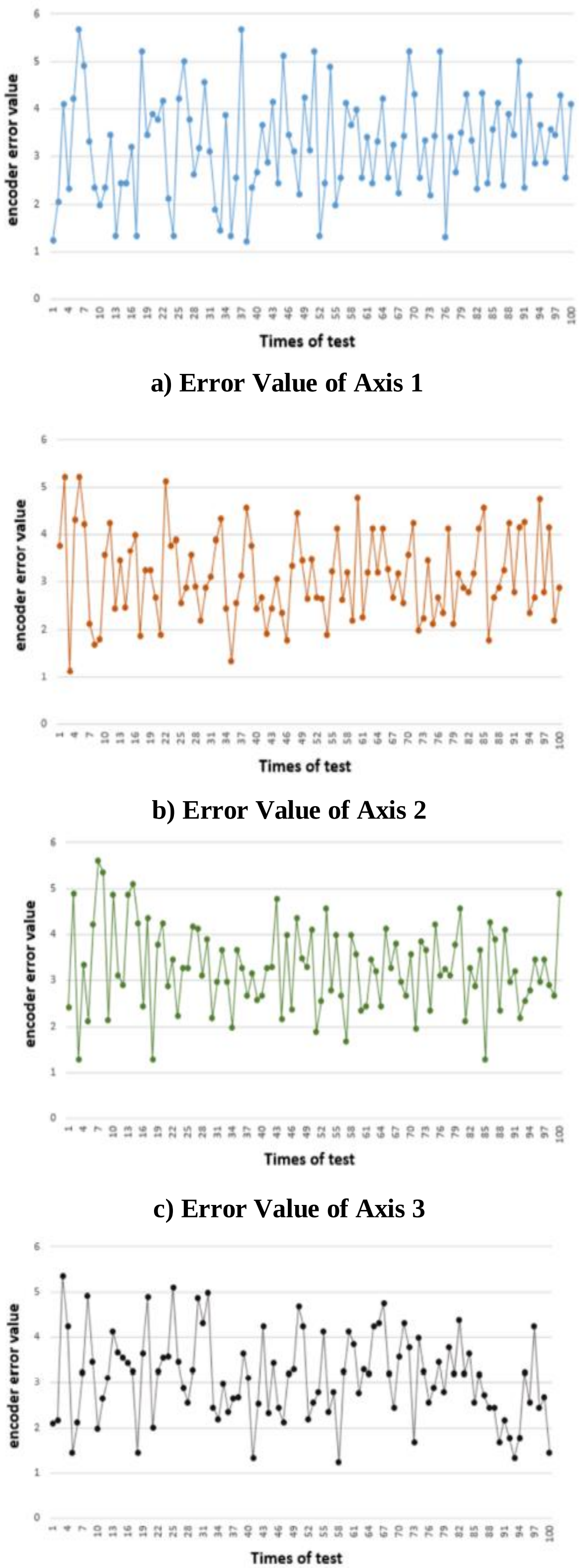

a) Error Value of Axis 1

b) Error Value of Axis 2

c) Error Value of Axis 3

d) Error Value of Axis 4

Fig. 9 Experimental with Articulated Robot Movements

IV. CONCLUSIONS

This Research described the articulated robotic arm by using the Denavit-Hartenberg model to control between loading and unloading of a ceramic to the kiln. The performed device for the automatic robot arm that features are high performance and compared with the Simulink has been successful with joint angle configuration $\theta_1, \theta_2, \theta_3, \theta_4$. At the same time, the control method got the different error values, and a little bit position error such as axis 1 is ±3.2451 mm, axis 2 is ±3.123 mm, axis 3 is ±3.2754 mm, and axis 4 is ±3.171 mm, respectively. In the future, loading and unloading of ceramic jobs is a requirement for automation that can reduce working time, reduce the damage to prevent the fracture of the workpiece as well as help and prevent danger while working with various models. The experimental relative and Simulink are very optimal that can run the articulated robotic arm to loading and unloading place the object effectively and automatic power a good behaviour in a ceramic plant and environment.

REFERENCES

[1] Ju. H.J, Zhao. Q, and Sun.X, Microwave oven design using HFSS simulation software, Material Review A 21(11) (2007) 237-239.

[2] Tian. M.B, Substrates for High-Density Package Engineering, Tsinghua University Press, Beijing, (2003) 22-24.

[3] Rao. Y, Wong. C.P, and Qu. J, Marins.T, A precise numerical prediction of effective dielectric constant for polymer ceramic based on effective medium theory, IEEE Tran. Comp. Packaging Technologies, 23 (2000) 680-683.

[4] Norton. F.H, Elements of Ceramics, Addison Wesley Publishing Company, INC, Massachusetts. (1957).

[5] Ding. X.W, Design and Implementation of an Automatic Ceramic Powder Weighing System, Foshan Ceramics, 12(12) (2002) 25-28.

[6] Wang. X, and Chen. Y, Research and Realization of Auto-Distribution Product System of Ceramics Based on USS Protocol, China Ceramic Industry, 10(6) (2003) 23-27.

[7] Wang. W.L, Zhu. F, and Zhu. W.Q, A Summary of Automation Technology Development for Ceramic Tile Production Line, China Ceramics, 42(1) (2006) 4-7.

[8] He. J, Zhang. C.F, and Long. Y.H, Research on a Method of Robust Controller Design and its Application, J. of Electronic Measurement and Instrument, 18(1) (2004) 6-11.

[9] Ji.E.K, Song.Y.H, Bak.S. H, Jung. M. K, Jeong. B. W, Lee. D. B, and Yoon. D. H, The Design of a ceramic phosphor plate with functional materials for application in high power LEDs, J. Mater. Chem. C, 3 (2015) 12390-12393.

[10] Liang. S, Control System Design and Kinematics Simulation of Six Degrees of Freedom Manipulator, Beijing industry University, (2009) 1-16.

[11] Yonglun. Cheng, Research and Simulation Analysis on kinematics of QJ-1 Welding Robot, Zhejiang University, (2008) 1-9.

[12] Wang. H. X, Lu. X, Sheng. C. Y, Zhang. Z. G, Cui. W, and Li. Y. X, General frame for arbitrary 3R subproblems based on the POE model, Robotics and Autonomous Systems, 105(138) (2018) 138-145.

[13] Park. I. W, Lee. B. J, Cho.. S. H, Hong. Y. D, and Kim. J. H, Laser-Based Kinematic Calibration of Robot Manipulator Using Differential Kinematics. IEEE/ASME Transactions on Mechatronics, 17(6) (2012) 1059-1067.

[14] Chen.T. Li, Chu. M, Jia. Q. X, and Sun. H. X, Review on kinematics calibration technology of serial robots, International Journal of Precision Engineering and Manufacturing, 15(8) (2014) 1759- 1774.

[15] John. J. C, Introduction to Robotics Mechanics and Control, Prentice Hall. (2005).

[16] Zhang. Q. Z, and Lan. Y, The technical renovation and Simulation of kiln temperature control system, Automation Technology and Its Application, China, 1 (2009) 34-37.

[17] Jinan. T, Design of multilayer ceramic package and its some question in the application, Electronics and packaging, 3(9) (2003) 28-33.

[18] Zhenya. L, and Zhao. Y, The status and future prospects of System in package technology, Electronics and packaging, 9(2) (2009) 5-10.

[19] Pavel. D, and Abdul. M. M, An advanced control technology for robotic palletising in materials handling for higher productivity, Proceedings, 15th International Conference on Mechatronics Technology, Melbourne, (2011) 100-105.

[20] Bechthold. M. et al., Integrated environmental Design and robotic fabrication workflow for ceramic shading systems, Proceedings of 28th International Symposium on Automation and Robotics in Construction (ISARC2011), Seoul, (2011).

Appendix A

Computer Programme

A. Flowchart of Control Program

The articulated robot arm with a four Degree of Freedom (4-DOF) has been designed to set between loading and unloading a ceramic to the kiln. The robot can be controlled by direct mechanical linkages from a remote point. Viewing is done through a window to protect the operator from hazards. These devices are used in the ceramic plant while handling dangerous substances. The robot used in the space shuttle is a mechanical manipulator controlled by a programmable logic controller through a computer link. Fig. 10. Shows a flowchart of the control program of the articulated robot arm of the present ceramic oven.

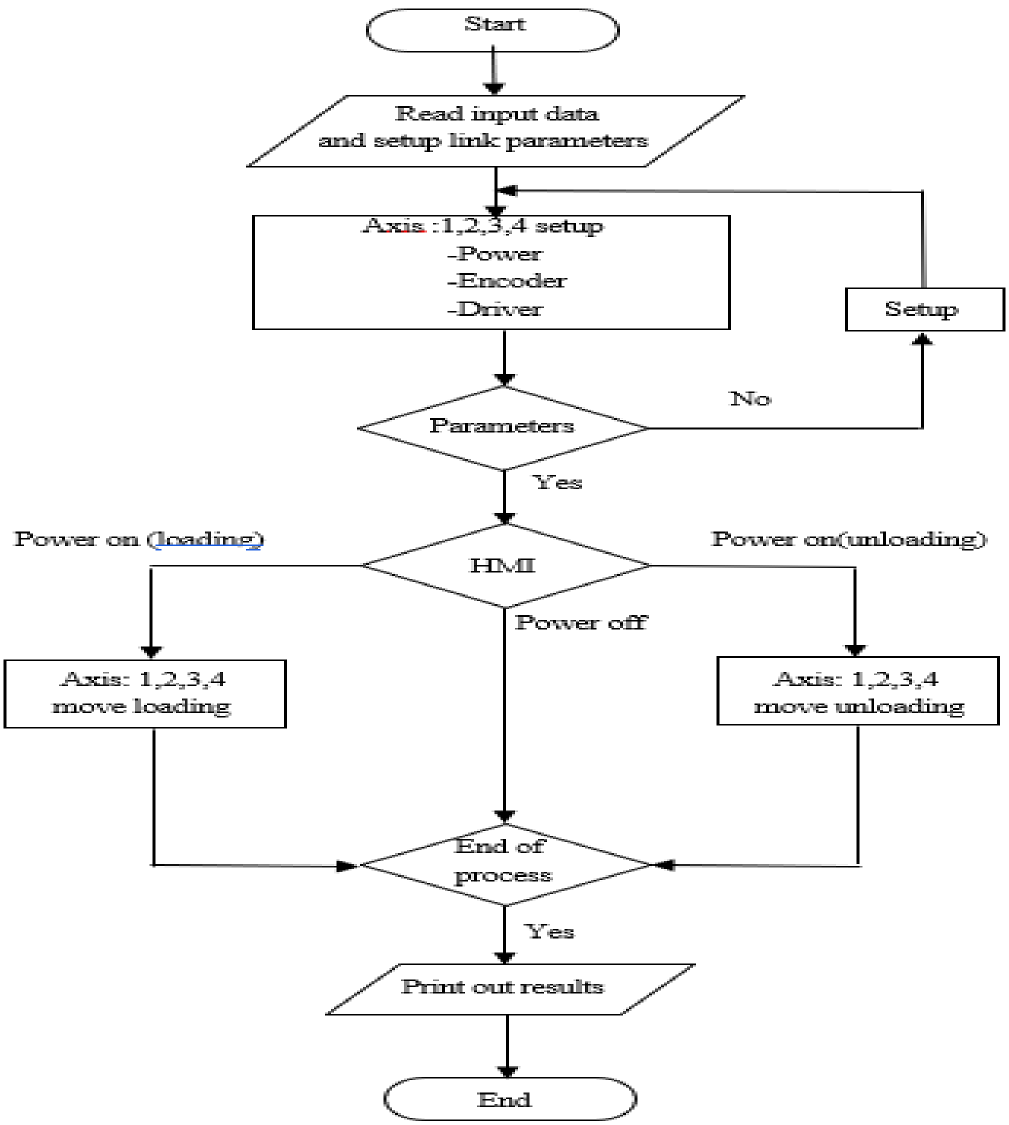

Fig. 10 Flowchart of the control program of present a ceramic kiln

B. Software Development

Software development of the articulated robotic arm has been using TwinCAT software. In this Research, the programming of this robot's motion control program is consists of three languages such as Ladder Diagram (LD), Function Box Diagram (FBD), and Structured Text (ST). Software development can be represented as follows:

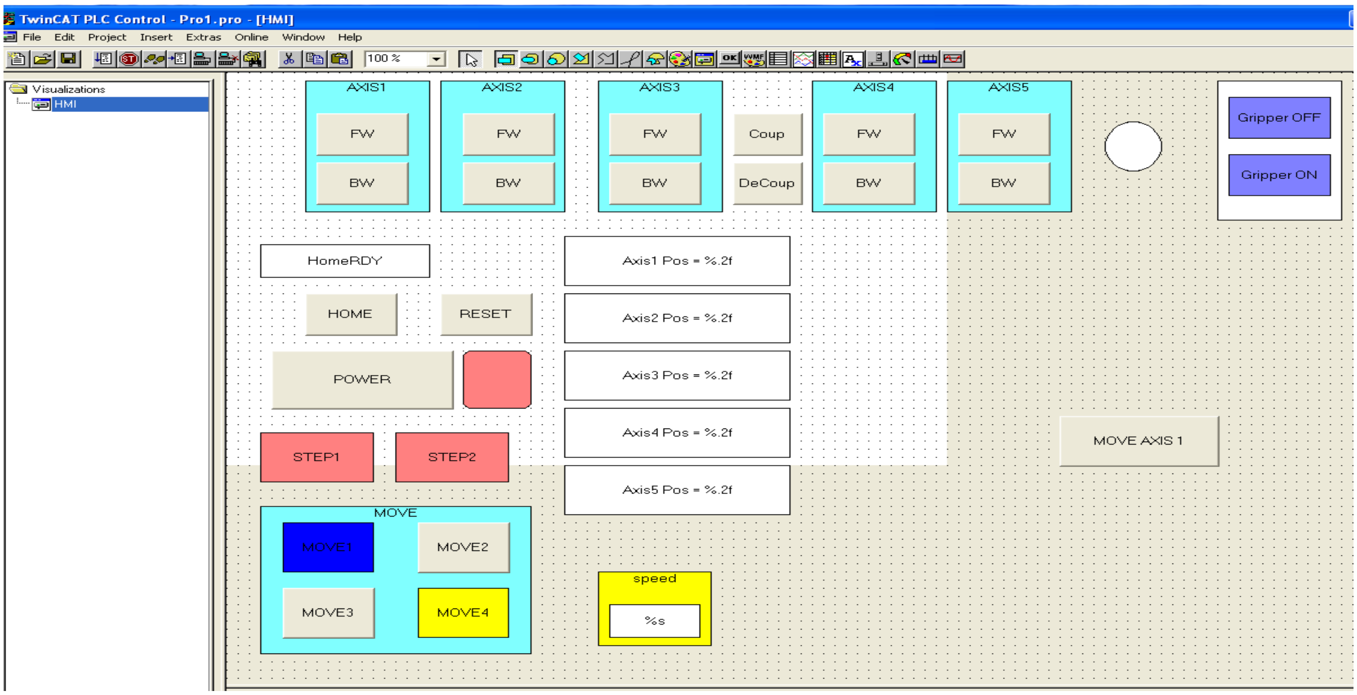

Fig. 11 TwinCAT system manager

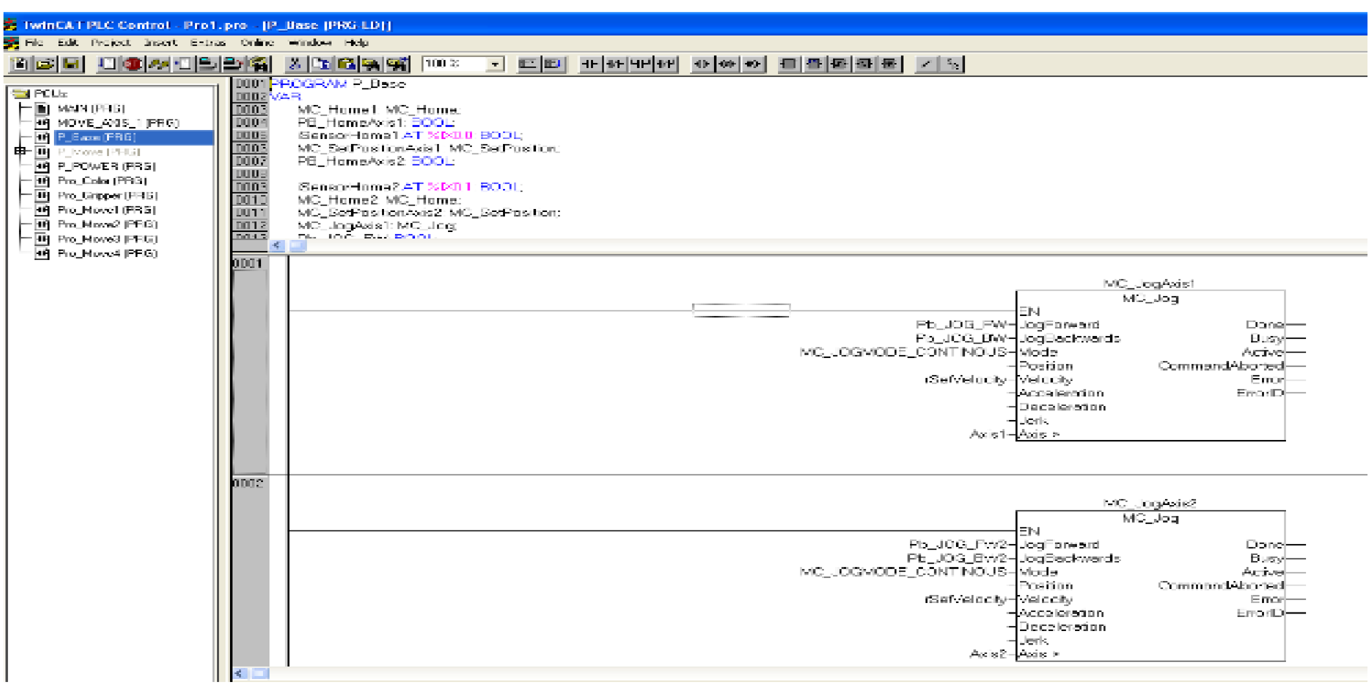

Fig. 12 HMI control

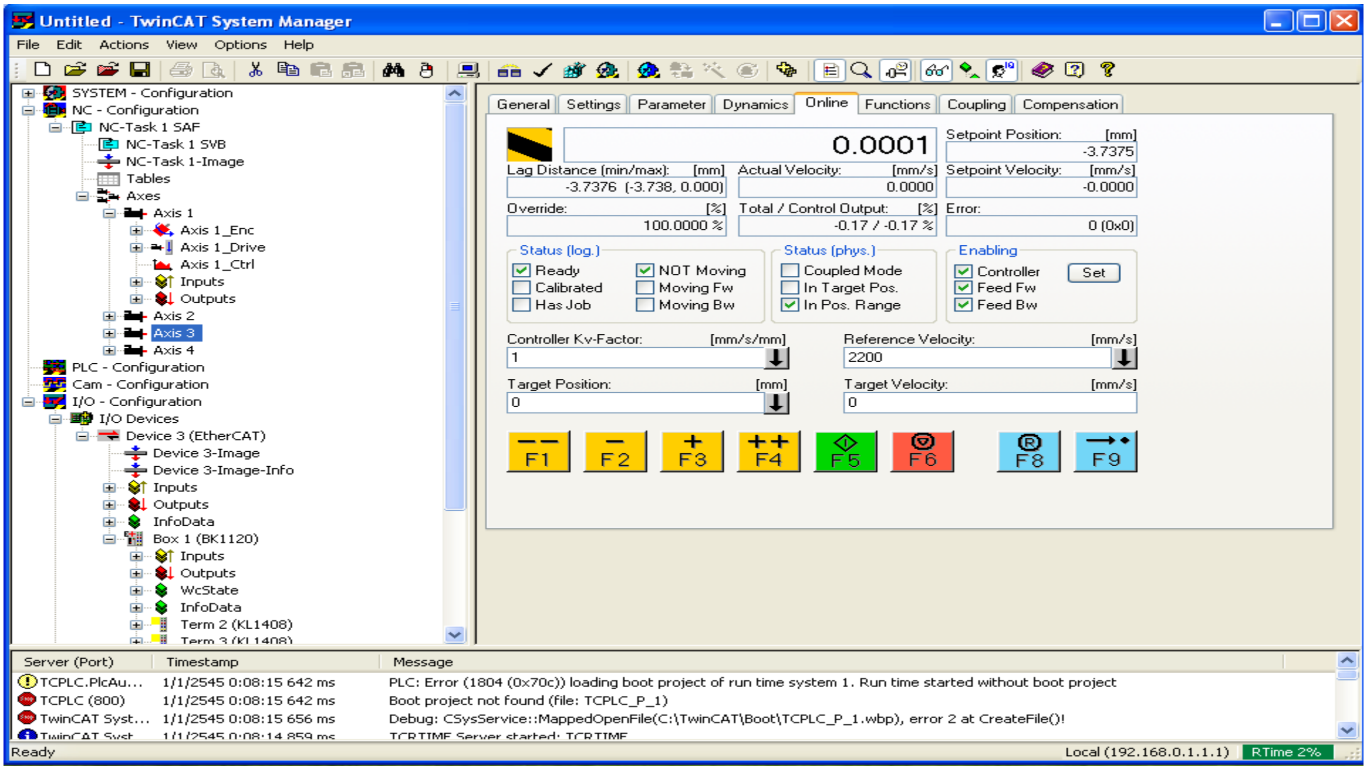

Fig. 13 Main Program at move axis

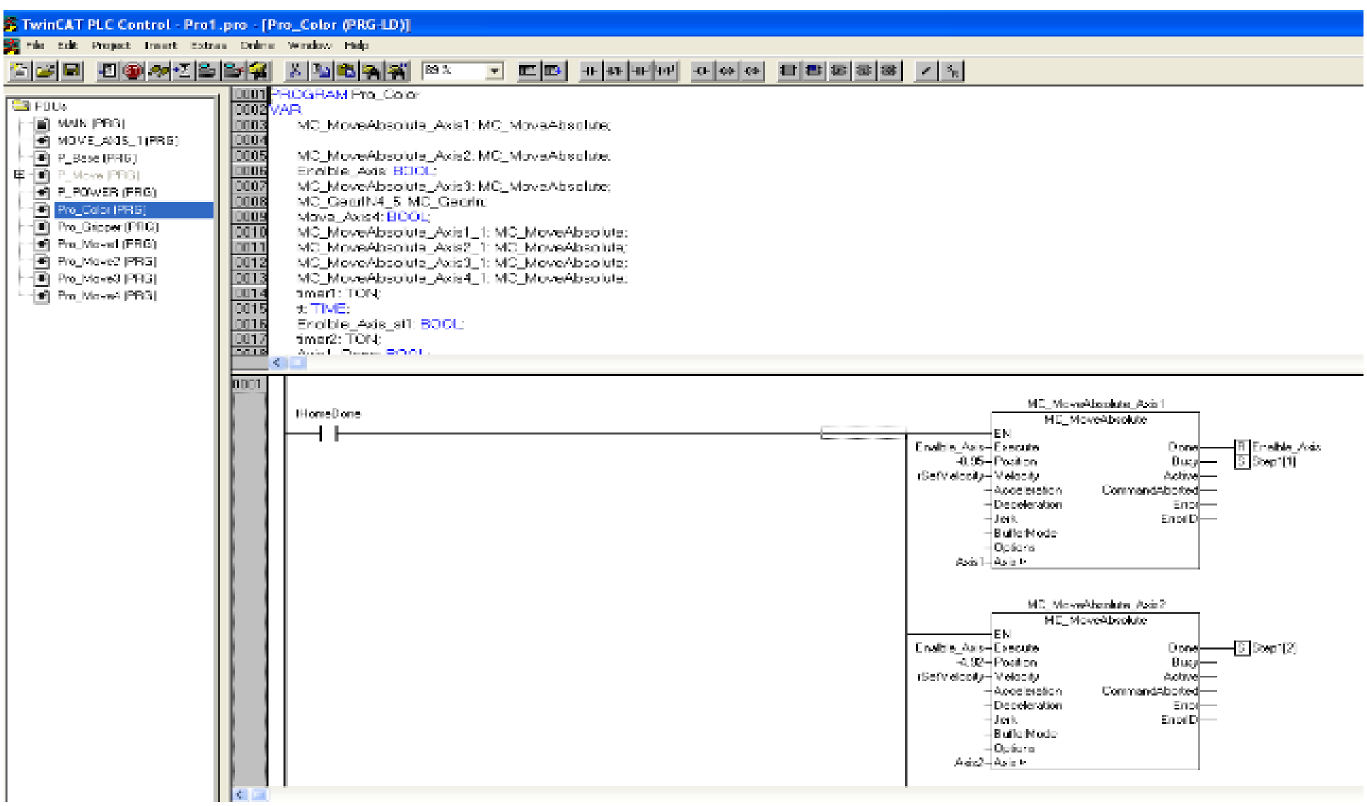

Fig. 14 Main Program at jog axis

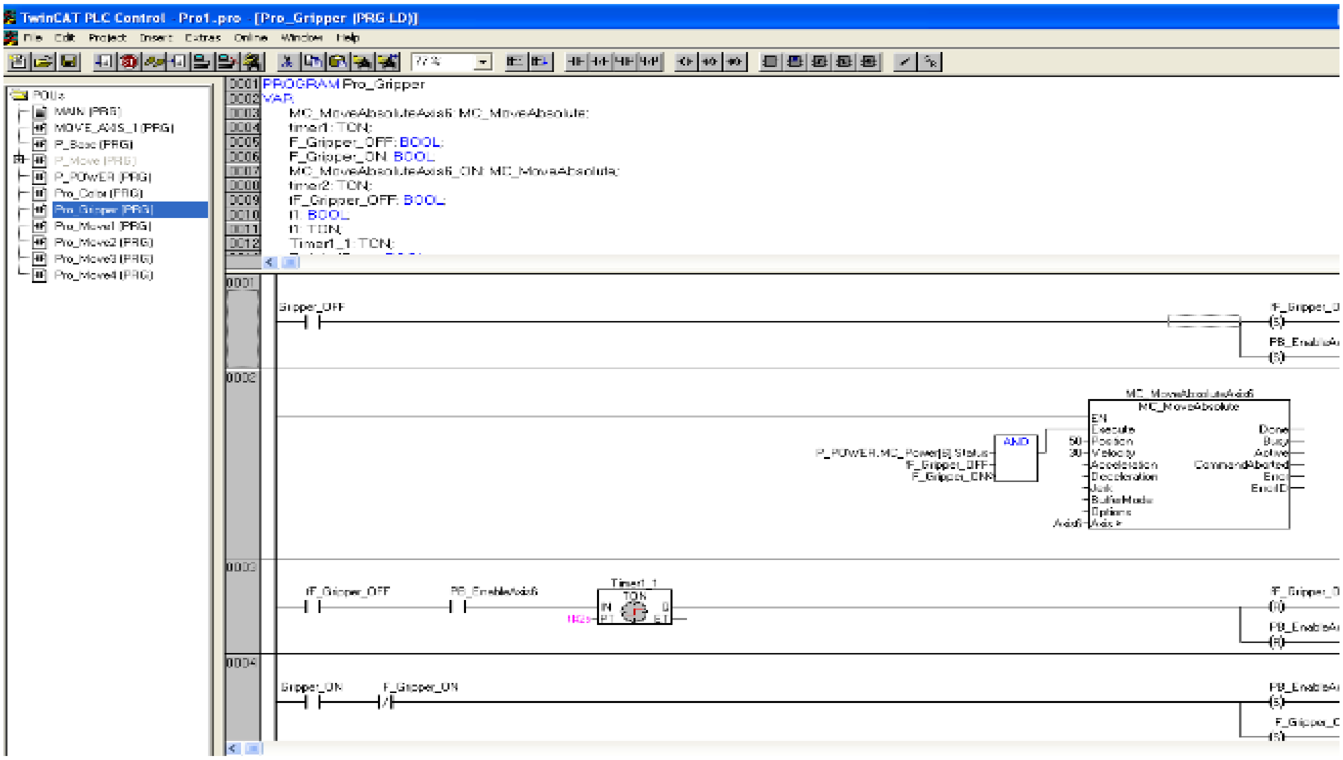

Fig. 15 Main Program at power

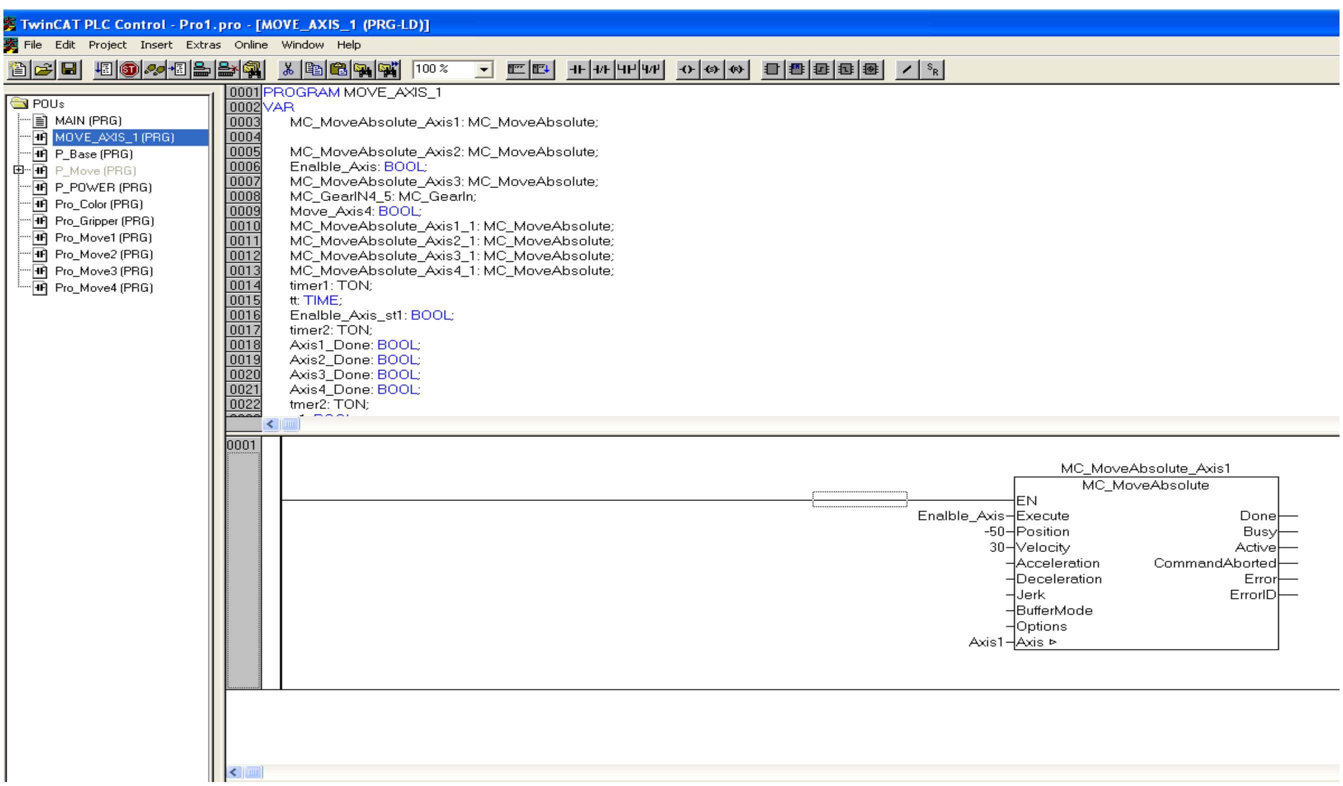

Fig. 16 Main Program at Move Absolute

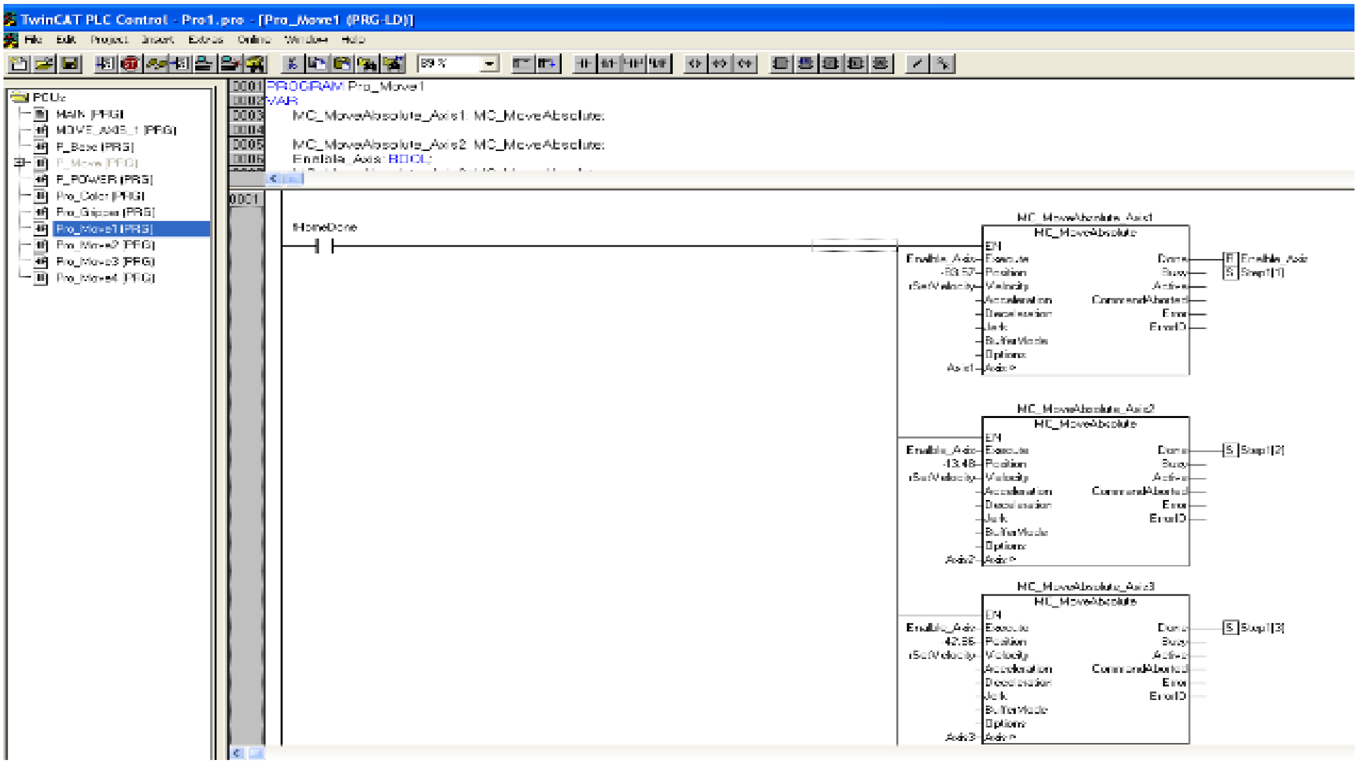

Fig. 17 Main Program at the Gripper

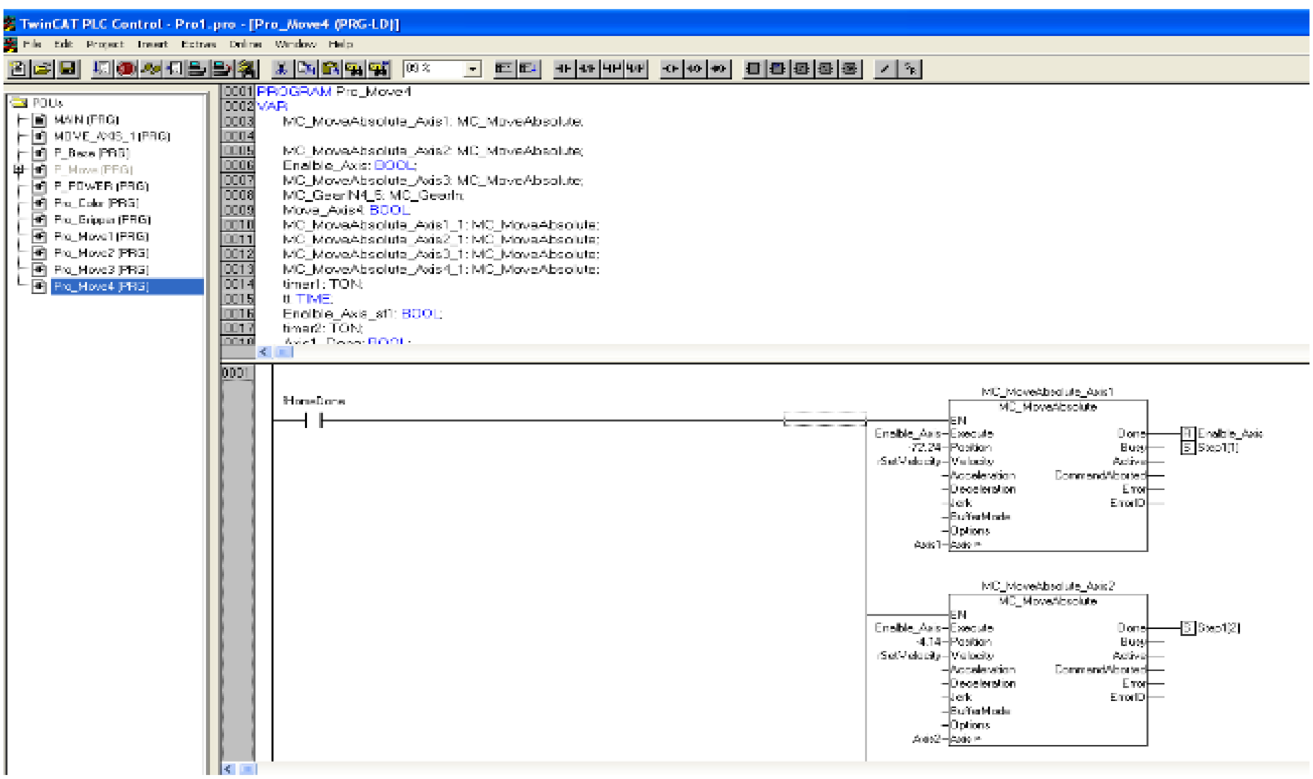

Fig. 18 Main Program at move1

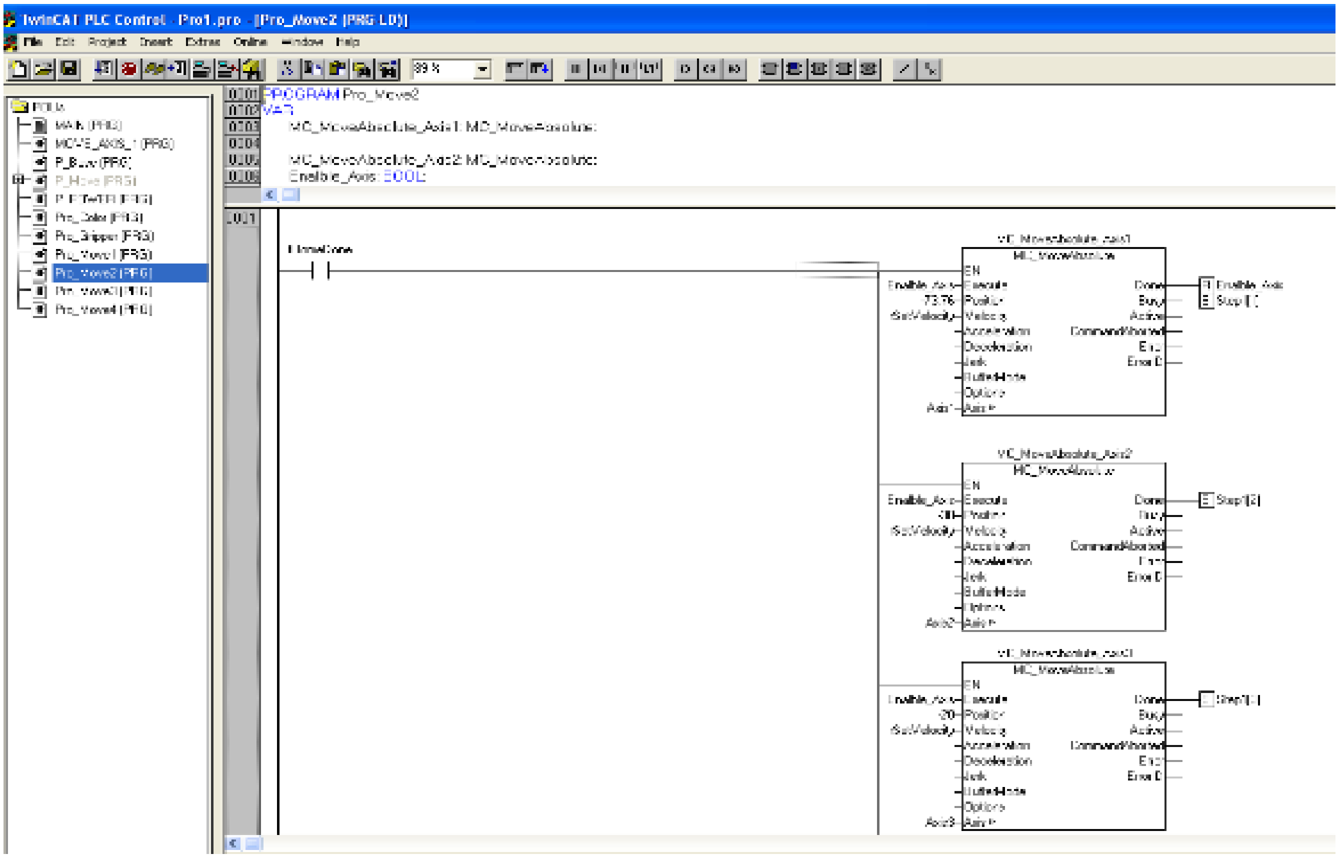

Fig. 19 Main Program at move 2

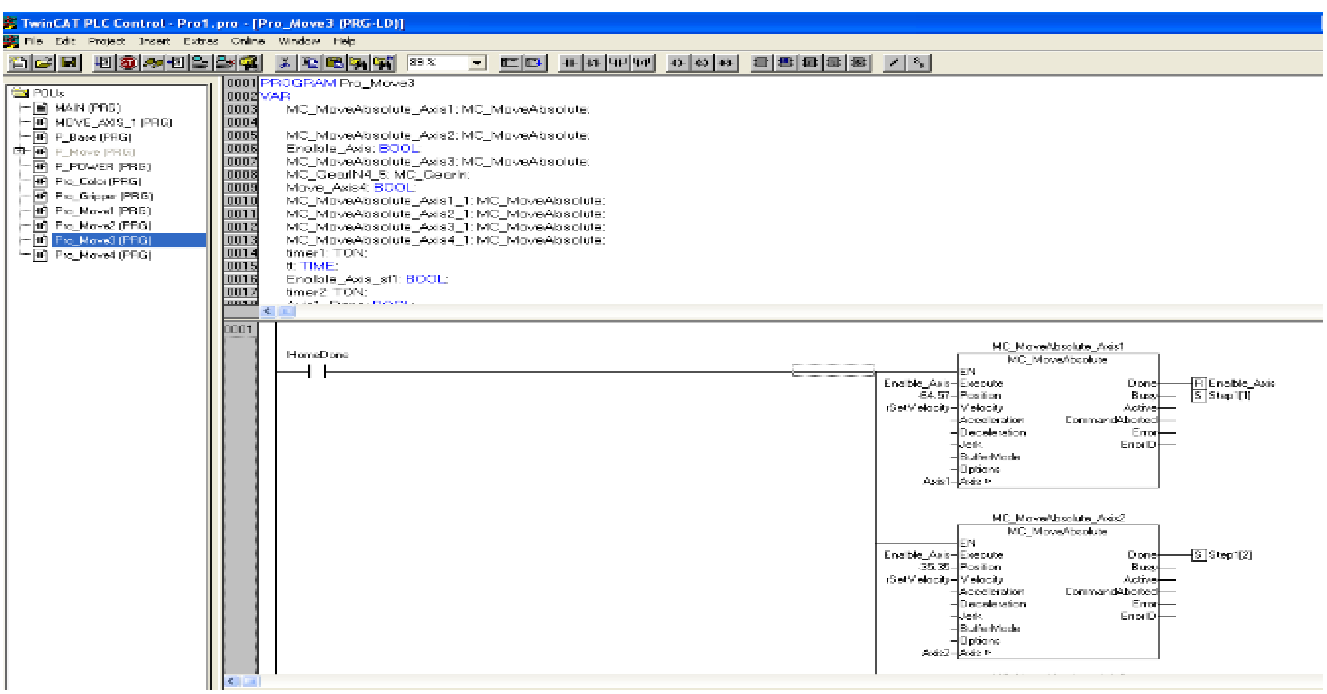

Fig. 20 Main Program at move 3

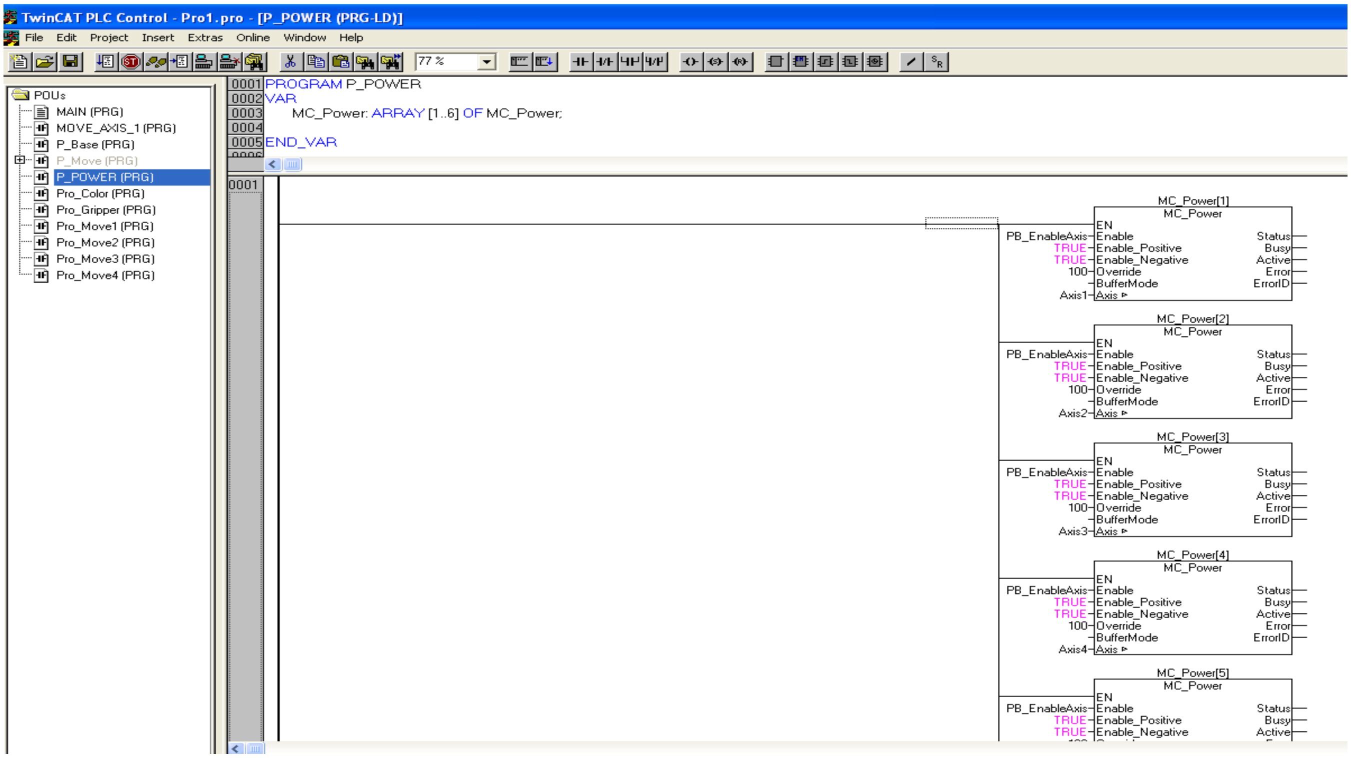

Fig. 21 Main Program at move 4